

# Influence of the Size and Type of Pores on Brick Resistance to Freeze-Thaw Cycles

---

**Netinger Grubeša, Ivanka; Vračević, Martina; Ducman, Vilma; Marković, Berislav; Szenti, Imre; Kukovecz, Akos**

*Source / Izvornik:* **Materials, 2020, 13, 3717 - 3729**

**Journal article, Published version**

**Rad u časopisu, Objavljena verzija rada (izdavačev PDF)**

<https://doi.org/10.3390/ma13173717>

*Permanent link / Trajna poveznica:* <https://urn.nsk.hr/urn:nbn:hr:133:760707>

*Rights / Prava:* [Attribution 4.0 International](#)/[Imenovanje 4.0 međunarodna](#)

*Download date / Datum preuzimanja:* **2025-02-05**



GRAĐEVINSKI I ARHITEKTONSKI FAKULTET OSIJEK  
Faculty of Civil Engineering and Architecture Osijek




*Repository / Repozitorij:*

[Repository GrAFOS - Repository of Faculty of Civil Engineering and Architecture Osijek](#)



Article

# Influence of the Size and Type of Pores on Brick Resistance to Freeze-Thaw Cycles

Ivanka Netinger Grubeša <sup>1,\*</sup>, Martina Vračević <sup>2,\*</sup> , Vilma Ducman <sup>3</sup> , Berislav Marković <sup>4</sup> , Imre Szenti <sup>5</sup> and Ákos Kukovecz <sup>5</sup>

<sup>1</sup> Faculty of Civil Engineering and Architecture Osijek, Josip Juraj Strossmayer University of Osijek, Vladimira Preloga 3, 31000 Osijek, Croatia

<sup>2</sup> Institute IGH, Janka Rakuše 1, 10000 Zagreb, Croatia

<sup>3</sup> Slovenian National Building and Civil Engineering Institute, Dimičeva Ulica 12, 1000 Ljubljana, Slovenia; vilma.ducman@zag.si

<sup>4</sup> Department of Chemistry, Josip Juraj Strossmayer University of Osijek, Ulica Cara Hadrijana 8/A, 31000 Osijek, Croatia; bmarkovi@kemija.unios.hr

<sup>5</sup> Interdisciplinary Excellence Centre, Department of Applied and Environmental Chemistry, University of Szeged, H-6720, Rerrich Béla tér 1, 6720 Szeged, Hungary; szentiimre@gmail.com (I.S.); kakos@chem.u-szeged.hu (Á.K.)

\* Correspondence: nivanka@gfos.hr (I.N.G.); martina.vracevic@igh.hr (M.V.)

Received: 29 June 2020; Accepted: 17 August 2020; Published: 22 August 2020



**Abstract:** This paper estimates the frost resistance of bricks using the ratio of compressive strength before freezing to compressive strength after freezing to describe the damage degree of bricks being exposed to freeze-thaw cycles. In an effort to find the ratio that clearly distinguishes resistant bricks from non-resistant bricks, the authors attempted to establish the correlation between the ratio and Maage factor as a recognized model for assessing brick resistance. To clarify the degree of damage of individual bricks, the pore size distribution has been investigated by means of mercury porosimetry. Additionally, micro computed X-ray tomography (micro-CT) has been employed to define the influence of the type of pores (open or closed) and their connectivity on the frost resistance of bricks. According to the results, it can be concluded that there is a good correlation between the Maage factor and the ratio of pre- to post-freeze-thaw cycle compressive strengths, and that the latter ratio strongly correlates with the percentage of large pores ( $\geq 3$  mm) in the brick. If such a correlation could be confirmed in a larger sample, then the ratio of pre- to post-freeze-thaw cycle compressive strengths could be used as a new method for assessing brick resistance to freeze-thaw cycles and it would be possible to determine the minimum percentage of large pores required to ensure the overall resistance of brick to freeze-thaw conditions. The complexity of the problem is, however, evidenced by the fact that no clear connection between the type (open versus closed) or connectivity of pores and the frost resistance of bricks could be revealed by micro-CT.

**Keywords:** clay bricks; resistance to freeze-thaw cycles; compressive strength; MIP; micro-CT; Maage factor

## 1. Introduction

One of the main demands of external bricks or brick wall elements used as building materials is durability. Degradation of brick properties is primarily caused by salt crystallization and the cyclic freezing and thawing of water in the material [1–4]. During freezing, the expansion of ice may cause the development of straining inside the material. If there is no space to accommodate the expansion and the incurred straining exceeds the strength of the brick, then damage and/or cracks will occur.

European regulations stipulate that the frost resistance of bricks be evaluated according to CEN/TS 772-22 [5], where wall samples are directly exposed to freeze-thaw cycles. Global literature, however, additionally mentions various other indirect procedures and limits/critical values for each procedure in order to grade the resistance of bricks to freeze-thaw cycles. Canadian and American standards, for example, use compressive strength, boiling absorption, the saturation coefficient and water absorption to grade the resistance of bricks to freeze-thaw cycles [4,6]. Another highly acknowledged indirect procedure to predict the resistance of bricks to freeze-thaw cycles is the Maage factor [7–10]. The Maage factor is a statistical model based on experimental results, and it includes two main variables: the total volume of pores (PV) and the proportion of pores of a certain diameter, i.e., pores larger than 3  $\mu\text{m}$  (P3), that are not fully saturated due to the meniscus effect. If there is a certain amount of space available in larger pores (larger than 3  $\mu\text{m}$ ), this can accommodate the pressure arising from ice formation. Maage states the following equation to obtain a coefficient of brick resistance to freeze-thaw cycles (Fc):  $Fc = 3.2 \times PV + 2.4 \times P3$ . The classification of results is as follows:  $Fc > 70$ —high probability that the material will be resistant to freeze-thaw cycles under severe climatic conditions;  $55 < Fc < 70$ —uncertain zone of freeze-thaw resistance; and  $Fc < 55$ —low probability that the material will be resistant to freeze-thaw cycles under severe climatic conditions.

Alongside this simpler model, there are two modified models designed by Korothe [1]. Korothe has, in one model, connected the total volume of pores in the brick with the boiling absorption, and, in the second one, connected the proportion of pores larger than 3  $\mu\text{m}$  in the brick with the boiling absorption, water absorption during a 1-h period and capillary absorption during exposure of the brick to water over a 4-h period. Conversely, Vincenzini [10] uses the critical radius of pores, F90, which is considered a 90% fractal, as a parameter to classify brick elements as resistant or non-resistant, while Franke and Bentrup [10] take the median radius of pores, F50. Litvan [11] estimates the resistance of bricks to freeze-thaw cycles based on the specific surface area of the pores, while Robinson [1,10] developed a coefficient based on the compressive strength, water absorption parameters and saturation coefficient. Arnott [10] defines the durability coefficients based on the strength and visual damage. Nakamura [10] developed three durability coefficients, one based on the physical properties of the brick elements, the second based on the specific volume of pores and a third based on a combination of the specific volume of pores and their distribution in the brick.

Each of the previously named procedures defines limit values where a brick is considered to be either resistant or non-resistant to freeze-thaw cycles, as well as the reliability of the method. Fagerlund [12] proved in his research that, if a brick sample is burdened by moisture under the critical point of saturation (“Scrit”), the same brick can be exposed to freeze cycles hundreds and thousands of times without any measurable damage. The point of saturation, Scrit, is reached when all of the open pores are saturated with moisture [12].

Consulting the previously identified reference literature, it can be seen that most of the authors consider porosity and the structure of pores to have a big influence on the durability properties of clay wall elements. Various research [1,6–11,13–18] suggests that the size of pores and the distance between pores significantly influence the properties of durability. According to Nakamura [1], pores with a diameter under 0.2  $\mu\text{m}$  are not desirable for properties of durability. Arnott [1] claims that pores larger than 1–3  $\mu\text{m}$  are desirable for durable properties of a clay product. According to Korothe and Maage, the estimation of the freezing durability is based not only on the total volume but also on the number of pores larger than 3  $\mu\text{m}$ , which are easily filled and emptied of water and as such improve the durability properties of the brick [1,7–10].

In order to assess a clay product’s resistance to freeze/thaw cycles, researchers have been studying the changes of the following properties during freeze/thaw cycles: the surface appearance of the specimens [4,19–21], flexural strength and toughness [20], compressive strength and dynamic modulus of elasticity [22], propagation speed of ultrasonic waves through specimens [18,22], weight of specimens [21–24] and structure of pores [20].

It is evident from the literature cited in the previous paragraph that researchers rarely evaluate the resistance of bricks to freeze-thaw cycles by studying changes in compressive strength. Therefore, the authors of this paper decided to focus precisely on this brick property. The degree of brick damage experienced during the freeze-thaw cycles is observed here through the ratio of compressive strength before freezing to compressive strength after freezing. In an effort to find the ratio that clearly distinguishes resistant from non-resistant bricks, the authors attempted to establish the correlation between the ratio and the Maage factor as a recognized model for assessing brick resistance. To clarify the degree of damage of individual bricks, the pore size distribution has been investigated by means of mercury porosimetry. Additionally, micro computed X-ray tomography (micro-CT) has been employed to define the influence of the type of pores (open or closed) and their connectivity on the frost resistance of bricks.

## 2. Materials and Methods

### *Description of Testing Methods*

Eight series of commercially available factory-made bricks were sampled from building material depots in Croatia, Bosnia and Herzegovina, and Serbia, named here as S1–S8. Although European regulations test the resistance of bricks to freeze-thaw cycles according to CEN/TS 772-22 [5], the direct resistance of bricks to freeze-thaw cycles was tested here according to the standard HRN B.D8.011 [25] on four sets of bricks (one set is comprised of five bricks) within each brick series. Under the chosen standard, the samples were saturated with water and exposed to temperatures of  $-20 \pm 2$  °C for four hours in a climate chamber. The samples were subsequently submerged in water at a temperature of  $+15$ – $20$  °C, also for four hours. This cycle was repeated 25 times, and the brick was considered durable to freeze-thaw cycles if there were no signs of damage in any of the examined samples after 25 cycles of freezing and then defrosting in water. Both of the above assessment methods yield a solely qualitative grade for brick resistance to freeze-thaw cycles. Unlike in CEN/TS 772-22 [5], where brick resistance is tested by looking at a brick as part of a wall, in HRN B.D8.011 [25] the resistance of a brick is viewed by looking at the brick as a test unit and is thus more severe. After the bricks were exposed to freeze-thaw cycles according to HRN B.D8.011 [25], their compressive strength was determined, and the results were compared to the compressive strength of bricks from the same series which had not been exposed to the freeze-thaw cycles. In this way, a ratio between the compressive strengths before and after the freeze-thaw cycles was acquired as a quantitative indicator of the brick resistance to freeze-thaw behavior. The compressive strength before and after freezing was measured according to EN 772-1 [26] on ten brick samples (one brick sample was comprised of two brick units). Before testing, the surface of all specimens was prepared by grinding until the requirement for planeness and parallelism given in EN 772-1 [26] was achieved, and the specimens were conditioned (dried) at  $105 \pm 5$  °C to a constant mass.

The structure of pores, their distribution, total porosity, the median radius of pores and the total pore volume (PV) of the bricks was determined using a Micromeritics AutoPore IV 9500 mercury intrusion porosimeter (MIP, Micromeritics, Norcross, GA, USA). For this test, fragments of brick with dimensions of approximately  $1 \text{ cm}^3$  were cut from each sample, dried for 24 h at 70 °C, degassed and then tested with mercury. Under high pressure (from 0 to 318 MPa), Hg penetrates into porous samples, and this gives information about the total open porosity as well as the pore size distribution. All the parameters determined by MIP were measured on three samples of each brick series.

The distribution of pores in the samples was also obtained via X-ray micro-computed tomography analysis, conducted using a Bruker Skyscan 2211 unit. Samples (Bruker, Kontich, Belgium) with a dimension of  $\sim 2.0 \times 2.0 \times 2.0 \text{ mm}^3$  were scanned using an 11 Mp cooled CCD (charge coupled device) camera using a source voltage of 100 kV, a source current of 400  $\mu\text{A}$  and an exposure time of 300 ms. The voxel size of this dataset was  $0.4 \times 0.4 \times 0.4 \text{ }\mu\text{m}$ . NRecon reconstruction software ((version 1.7.3.0)) was used to reconstruct the projected images with a pixel size of  $4032 \times 2688$ , and CTan (version 1.18) and CTvol (version 2.0) software were used to represent the 3D models. This device scopes pores

sized 2–100  $\mu\text{m}$ . The parameters determined by X-ray micro-computed tomography were obtained by measuring each type of brick sample three times, and the calculations were performed on several different volumes of interest (VOI). Example of cross-sectional slice as measured by micro-CT and the corresponding processed binary image used in the quantitative image analysis are given in Figure S1 of Supplementary materials.

### 3. Results

#### 3.1. Assessment of Frost Resistance Using the Direct Method

Seven out of the eight brick series exposed to 25 freeze-thaw cycles experienced some form of damage, either cracking or delamination. The typical appearance of the brick samples after their exposure to the freeze-thaw cycles is shown in Figure 1a,b.



**Figure 1.** Typical appearance of non-resistant bricks after 25 freeze-thaw cycles, (a) damage in the form of cracking; (b) damage in the form of delamination.

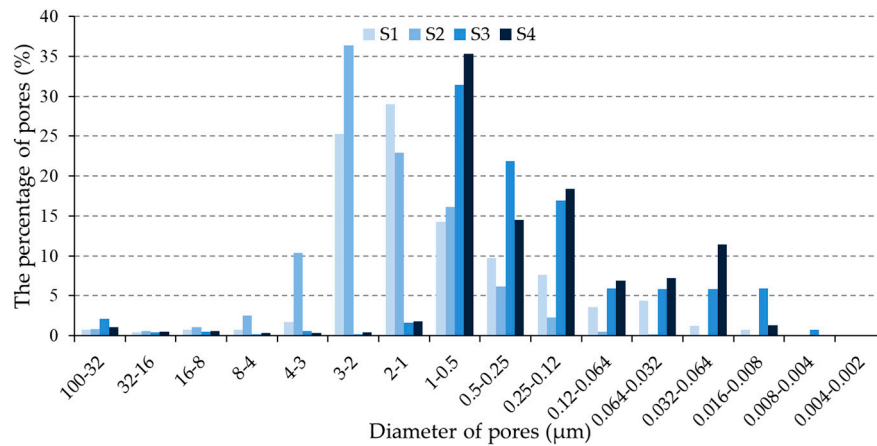
In accordance with HRN B.D8.01, a brick is deemed to be resistant to freeze-thaw cycles if, after 25 cycles of freezing at  $-20\text{ }^{\circ}\text{C}$  followed by thawing in water, no sample show signs of damage. According to these criteria, only the S7 brick was shown to be resistant to freeze-thaw cycles, with the rest of the bricks being classified as non-resistant. The compressive strength of the bricks before and after freeze-thaw cycles with the corresponding standard deviation, as well as the ratio between the pre- and post-freeze-thaw cycle compressive strengths, are shown in Table 1. The compressive strengths (pre- and post-freezing) given here are the average values of ten individual measurements. The ratio of pre- to post-freezing compressive strengths was calculated by using the average values of the compressive strengths pre- to post-freezing.

**Table 1.** Compressive strength of bricks before and after freezing with the corresponding standard deviation and the ratio of compressive strengths pre- to post-freezing.

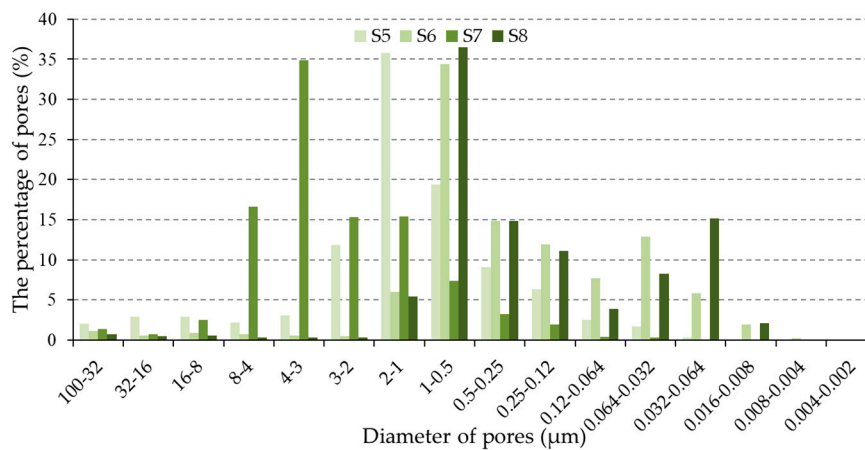
Brick Series/Property Tested	S1	S2	S3	S4	S5	S6	S7	S8
Normative compressive strength before freezing ( $\text{N}/\text{mm}^2$ )	$17.7 \pm 0.4$	$8.0 \pm 0.2$	$28.7 \pm 0.6$	$28.4 \pm 0.4$	$15.2 \pm 0.2$	$27.9 \pm 0.3$	$27.7 \pm 0.3$	$27.8 \pm 0.3$
Normative compressive strength after freezing ( $\text{N}/\text{mm}^2$ )	$12.1 \pm 0.3$	$5.6 \pm 0.1$	$20.4 \pm 0.4$	$19.70 \pm 0.3$	$10.9 \pm 0.2$	$18.9 \pm 0.3$	$24.6 \pm 0.3$	$19.13 \pm 0.3$
The ratio of compressive strength before freezing to compressive strength after freezing	0.68	0.70	0.71	0.69	0.72	0.68	0.89	0.69

### 3.2. Porosity and Pore Size Distribution

All the parameters determined by MIP were measured on three samples of each brick series, and considering the fact that the results of the three measurements were close to each other, the results given in Figure 2a,b and Table 2 present one sample, selected to be representative of a particular brick series. Figure 2a,b presents the pore size distribution in the brick series.



(a)



(b)

**Figure 2.** Pore size distribution in the brick series; (a) pore size distribution in brick series S1–S4; (b) pore size distribution in brick series S5–S8.

**Table 2.** Proportion of pores of a given size, total porosity, median pore radius and total pore volume in the bricks.

Property/ Brick Series	Proportion of Pores of a Given Size (%)			Total Porosity (%)	Median Pore Radius (mm)	Total Volume of Pores, PV (cm <sup>3</sup> /g)
	Large	Medium	Small			
S1	4.2	85.9	9.9	37.7	0.25	232.5
S2	15.4	83.9	0.7	46.11	1.01	370.5
S3	3.8	71.9	24.3	30.07	0.26	168.5
S4	2.8	70.4	26.8	30.77	0.08	171.2
S5	13.1	82.4	4.5	28.86	0.51	154.3
S6	3.9	67.6	28.5	32.99	0.09	183.2
S7	56.1	43.2	0.7	34.42	1.45	207.5
S8	2.4	68.1	29.5	32.34	0.05	813.3

In the reference literature [1,14], pores smaller than  $0.1\ \mu\text{m}$  are considered to be small, while pores in the range of  $0.1\text{--}1.0\ \mu\text{m}$  are considered to be medium-sized pores. According to Maage [7–10] and some other authors [6–9,13,27,28], large pores are larger than  $3\ \mu\text{m}$ . In line with this, pores were categorized by size into groups of large, medium and small, as shown in Table 2. The median pore radius, total porosity and total pore volume, as measured by MIP, are also shown in Table 2.

### 3.3. Micro-CT Investigations

The applicability of micro-CT to freeze-thaw resistance analysis in mortars has recently been demonstrated [29]. Here, this method has been extended to the characterization of bricks, with the results being shown in Figure 3 and tabulated in Table 3. Open cylindrical volumes of interest (VOIs), used for the quantitative analysis of reconstructed images (Figure 3), were individually optimized for each sample to ensure the optimal representation of the heterogeneous pore structure in the VOI-based calculations. Closed pores are marked here in red, open pores in blue, and the matrix is colored grey. It is well-observable that the samples exhibit considerable variety in both the percentage and the spatial distribution of open and closed pores. The open/closed pore ratio ranges from 0.25 (S8) to 136 (S2). This factor of a  $\times 500$  difference is significantly higher than the total porosity percentage range, which barely spans a factor of  $\times 6$  ( $4.18\%$  in S4 vs.  $23.28\%$  in S2). This indicates that pore connectivity is a complex characteristic of the samples that can only be interpreted in a three-dimensional context, as made available by micro-CT. It is worth noting that the trends observable from these micro-CT studies are in good qualitative agreement with the MIP results discussed below.

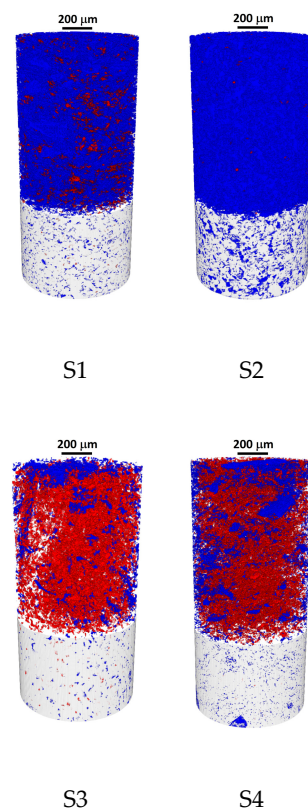
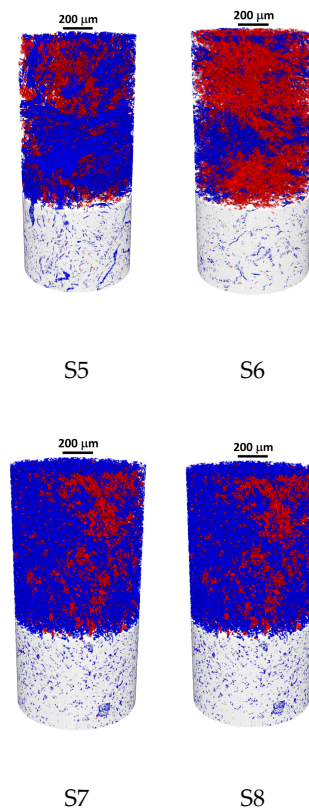


Figure 3. Cont.



**Figure 3.** Characteristic micro-CT images of brick samples illustrating the quantitative differences reported in Table 3 (closed pores are marked in red, open pores in blue and the matrix is colored grey).

**Table 3.** The percentage of open pores, the percentage of closed pores and the interconnection of pores.

Brick Series/Property Tested	S1	S2	S3	S4	S5	S6	S7	S8
The percentage of open pores (%)	11.95	23.11	1.42	1.13	8.51	2.52	16.01	0.92
The percentage of closed pores (%)	0.85	0.17	2.56	3.05	1.43	2.34	0.41	3.61
The total percentage of pores (%)	12.8	23.28	3.98	4.18	9.94	4.86	16.42	4.53
Interconnection of pores ( $\text{mm}^{-3}$ )	188,227	268,300	30,930	108,688	162,121	131,387	155,587	59,451

#### 4. Discussion

The results of the brick tests regarding their resistance to freeze-thaw cycles obtained by HRN B.D8.011, the estimation based on the ratio of compression strengths after and before freezing, and the estimation based on the Maage factor are summarized in Table 4.

Figure 4 shows the relationship between the Maage factor and the ratio of the compressive strength before freezing to that after freezing for the series of bricks observed in the present study. Mallidi [30], who has surveyed numerous studies focused on the parameters influencing frost resistance, concluded that the Maage factor is one the most reliable indices for predicting the durability of bricks. However, for such an assessment, mercury intrusion porosimetry is necessary. Considering the limited availability of this method, there is a need to find links between the pore and absorption characteristics of bricks, or a way to evaluate durability in other terms, for example as a ratio of the pre- to post-freezing compressive strengths. A good relation between the Maage factor and the ratio of the pre- to post-freezing cycle compressive strengths was observed in the case of the machine-made bricks in [31]. In Figure 4, it can be seen that these two variables (Maage factor and the ratio of pre- to post-freezing compressive strengths) are strongly correlated, as seen by a high linear fit  $R^2$  value of 0.99. The equation describing their relationship is  $y = 555.52 \times x - 353.73$ , where  $x$  is the ratio of the compressive strength before freezing to that after freezing and  $y$  is the Maage factor. If a value of 70, which is the lower limit of the



Maage factor at which bricks are considered to be resistant to freeze-thaw cycles, is introduced into this equation, one can calculate that the ratio of the compressive strength before to that after freezing must be at least 0.76 in order for bricks to be considered resistant to freeze-thaw conditions. If the ratio of the pre- to post-freezing compressive strengths is to be used as an indicator of the resistance of brick to freeze-thaw cycles, then a larger database will be needed in order to firmly identify classification limits. The authors of this paper will focus their future efforts in this direction.

**Table 4.** Summarized results of the methods applied to test brick resistance to freeze-thaw cycles.

Brick Series/Property Tested	S1	S2	S3	S4	S5	S6	S7	S8
Resistance according to HRN B.D8.011	Non-resistant	Non-resistant	Non-resistant	Non-resistant	Non-resistant	Non-resistant	Resistant	Non-resistant
The ratio of pre- to post-freezing compressive strengths	0.68	0.70	0.71	0.69	0.72	0.68	0.89	0.69
The Maage factor; estimation of resistance based on the Maage factor	24.0—low probability of resistance	41.0—low probability of resistance	42.0—low probability of resistance	28.0—low probability of resistance	53.0—low probability of resistance	19.0—low probability of resistance	139.0—high probability of resistance	24.0—low probability of resistance

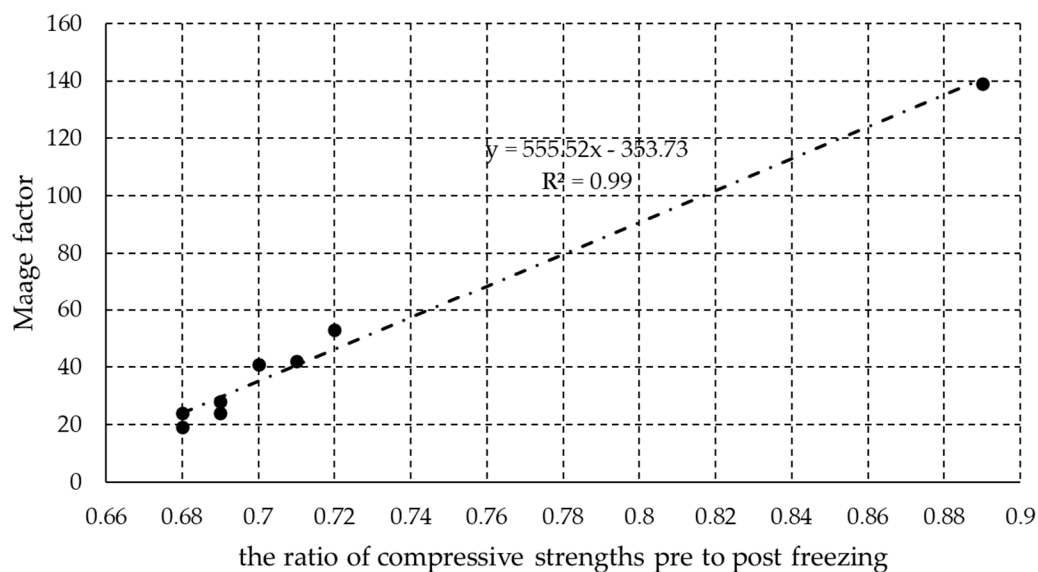


**Figure 4.** Correlation between the Maage factor and the ratio of pre- to post-freezing compressive strengths.

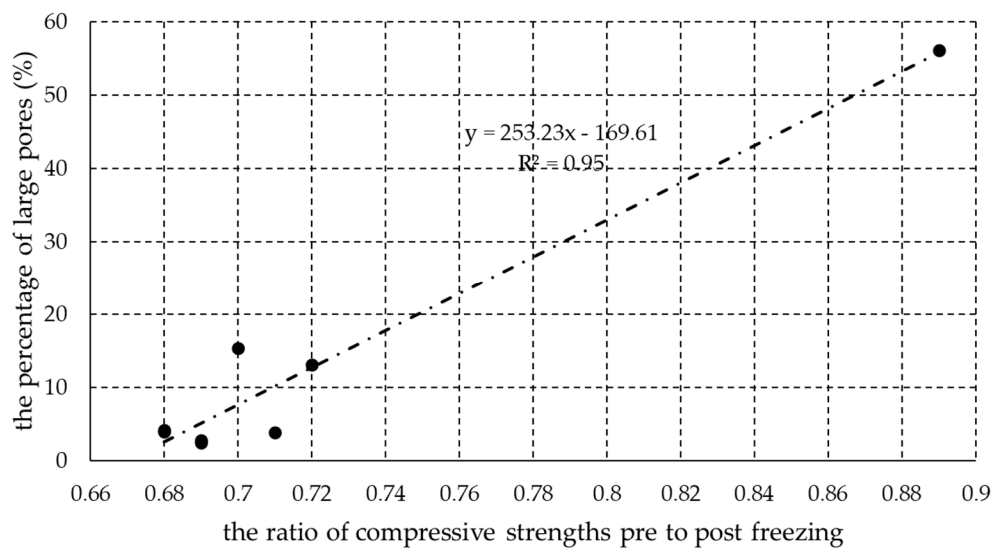
Furthermore, in an effort to find an answer to the effects of the pore size and type (open or closed), as well as their interconnection, on the resistance of brick to freeze-thaw cycles, these parameters are again extracted in Table 5.

**Table 5.** Summarized results of the brick resistance to freeze-thaw cycles, porosimetry and micro-CT.

Brick Series/Property Tested	S1	S2	S3	S4	S5	S6	S7	S8	
The ratio of the compressive strength before to that after freezing	0.68	0.70	0.71	0.69	0.72	0.68	0.89	0.69	
MIP results	The percentage of large pores (%)	4.2	15.4	3.8	2.8	13.1	3.9	56.1	2.4
	The percentage of medium pores (%)	85.9	83.9	71.9	70.4	82.4	67.6	43.2	68.1
	The percentage of small pores (%)	9.9	0.7	24.3	26.8	4.5	28.5	0.7	29.5
	The total percentage of pores (%)	37.7	46.11	30.07	30.77	28.86	32.99	34.42	32.34
	Median radius of the pores (mm)	0.25	1.01	0.26	0.08	0.51	0.09	1.45	0.05
micro-CT results	The percentage of open pores (%)	11.95	23.11	1.42	1.13	8.51	2.52	16.01	0.92
	The percentage of closed pores (%)	0.85	0.17	2.56	3.05	1.43	2.34	0.41	3.61
	The total percentage of pores (%)	12.8	23.28	3.98	4.18	9.94	4.86	16.42	4.53
	Interconnection of pores (mm <sup>-3</sup> )	188,227	268,300	30,930	108,688	162,121	131,387	155,587	59,451

Table 5 shows that the ratios of the pre- to post-freezing compressive strengths correlate very well with the percentage of large pores.

In Figure 5, it can be seen that these two variables are linearly correlated, with an R<sup>2</sup> value of 0.95. The equation describing their relationship is  $y = 253.23x - 169.61$ , where  $x$  is the ratio of the compressive strength before to that after freezing, and  $y$  is the percentage of large pores. In the previous step, it was suggested that a value of 0.76 could be used as a lower limit for the pre- to post-freezing compressive strength ratio in order to classify a brick as being freeze-thaw resistant. Taking this value forward to the second linear equation, we can further estimate that the percentage of large pores should be at least 23% for the brick to be considered as being resistant to freeze-thaw cycles.

**Figure 5.** Correlation between the percentage of large pores and the ratio of pre- to post-freezing compressive strengths.

The total porosity of bricks, as determined by tomography, is lower than the porosity determined by MIP. This is to be expected given a certain limitation of tomography, which, in the present case, can only detect pores bigger than 2  $\mu\text{m}$ , whereas MIP measurements can detect pores as small as 0.0055  $\mu\text{m}$ , consequently giving a higher porosity result [32]. The tomography results presented here indicate no clear connection between either the type of pores (open or closed) or their connectivity and the frost resistance of bricks. This is readily explained by the three orders of magnitude of difference in the lowest pore diameter range, as measured by MIP and micro-CT. Work is in progress

in our laboratory to address this complex problem from another aspect, e.g., via a micro-CT spatial inhomogeneity analysis.

## 5. Conclusions

This paper estimates the frost resistance of bricks using the ratio of the compressive strength before freezing to the compressive strength after freezing to describe the damage degree of bricks being exposed to freeze-thaw cycles. In an effort to find the ratio that clearly distinguishes resistant from non-resistant bricks, the authors attempted to establish the correlation between the ratio and the Maage factor as a recognized model for assessing brick resistance. To clarify the degree of damage of individual bricks, the pore size distribution was investigated by means of mercury porosimetry. Additionally, micro computed X-ray tomography (micro-CT) was employed to define the influence of the type of pores (open or closed) and their connectivity on the frost resistance of bricks. By analyzing the research results, the following conclusions could be made:

- A strong relationship was observed between the Maage factor and the ratio of the compressive strength before to that after freeze-thaw cycles. If such a correlation is confirmed on a larger sample, the ratio of the compressive strength before to that after freeze-thaw cycles could be used as a new method for assessing brick resistance to freezing and thawing.
- The ratios of the compressive strength before to that after freezing correlate very well with the percentage of large pores, meaning that further research in this direction might be able to determine the minimum percentage of large ( $\geq 3 \mu\text{m}$ ) pores required in order to ensure the overall resistance of brick to freeze-thaw cycles.
- In this research, no clear connection was observed between the type of pores (open or closed) or their connectivity and the frost resistance of bricks.

**Supplementary Materials:** The following are available online at <http://www.mdpi.com/1996-1944/13/17/3717/s1>, Figure S1. Example of cross-sectional slice as measured by micro-CT (a), and the corresponding processed binary image (b) used in the quantitative image analysis.

**Author Contributions:** Conceptualization, I.N.G. and M.V.; methodology, I.N.G., M.V., V.D., B.M., I.S. and Á.K.; formal analysis, I.N.G., M.V., V.D., B.M., I.S. and Á.K.; investigation, I.N.G., M.V., V.D., B.M., I.S. and Á.K.; resources, I.N.G., M.V. and Á.K.; writing—original draft preparation, I.N.G., M.V., V.D., B.M., I.S. and Á.K.; writing—review and editing, I.N.G., M.V., V.D., B.M., I.S. and Á.K. All authors have read and agreed to the published version of the manuscript.

**Funding:** Financial support from the Faculty of Civil Engineering and Architecture Osijek and Institute IGH as well as financial support from the Hungarian National Research, Development and Innovation Office through the projects GINOP-2.3.2-15-2016-00013 “Intelligent materials based on functional surfaces—from syntheses to applications”, GINOP-2.3.3-15-2016-00010 and 2018-2.1.12-TÉT-HR-2018-00009, and the Ministry of Human Capacities, Hungary, grant 20391-3/2018/FEKUSTRAT is acknowledged.

**Conflicts of Interest:** The authors declare no conflict of interest.

## References

1. Koroth, S.R. Evaluation and Improvement of Frost Durability of Clay Bricks. Ph.D. Thesis, Concordia University, Montreal, QC, Canada, 1997.
2. Abu Bakar, B.H.; Wan Ibrahim, M.H.; Megat Johari, M.A. A review: Durability of fired clay brick masonry wall due to salt attack. *Int. J. Integr. Eng.* **2011**, *1*, 111–127.
3. Mensinga, P. Determining the Critical Degree of Saturation of Brick Using Frost Dilatometry. Master’s Thesis, University of Waterloo, Waterloo, ON, Canada, 2009.
4. Netinger, I.; Vračević, M.; Ranogajec, J.; Vučetić, S. Evaluation of brick resistance to freeze/thaw cycles according to indirect procedures. *Gradevinar* **2014**, *66*, 197–209.
5. *Methods of Test for Masonry Units. Determination of Freeze/Thaw Resistance of Clay Masonry Units*; EN 772-22:2018; European Committee: Brussels, Belgium, 2018.

6. Vračević, M. A contribution to durability of masonry structures. Ph.D. Thesis, University J.J. Strossmayer, Faculty of Civil Engineering and Architecture Osijek, Osijek, Croatia, 2019. (In Croatian).
7. Dondi, M.; Marsigli, M.; Venturi, I. Microstructure and mechanical properties of clay bricks: Comparison between fast firing and traditional firing. *Br. Ceram. Trans.* **1999**, *98*, 12–18. [[CrossRef](#)]
8. Bracka, A.; Rusin, Z. Comparison of pore characteristics and water absorption in ceramics materials with frost resistance factor Fc. *Struct. Environ.* **2012**, *4*, 15–19.
9. Korenska, M.; Chobola, Z.; Sokolar, R.; Mikulkova, P.; Martinek, J.A.N. Frequency inspection as an assesment tool for the frost resistance of fired roof tiles. *Ceram. Silik.* **2006**, *50*, 185–192.
10. Raimondo, M.; Ceroni, C.; Dondi, M.; Guarini, G.; Marsigli, M.; Venturi, I.; Zanelli, C. Durability of clay roofing tiles: The influence of microstructural and compositional variables. *J. Eur. Ceram. Soc.* **2009**, *29*, 3121–3128. [[CrossRef](#)]
11. Litvan, G.G. *Testing the-Frost Susceptibility of Bricks*; ASTM STP 589; NRC Publications Archive: Ottawa, ON, Canada, 1975; pp. 123–132.
12. Straube, J.; Schumacher, C.; Mensinga, P. Assessing the freeze-thaw resistance of clay brick for interior insulation retrofit projects. In Proceedings of the XI International Conference Thermal Performance of the Exterior Envelopes of Whole Buildings, Clearwater, FL, USA, 5–9 December 2010.
13. Raimondo, M.; Dondi, M.; Gardini, D.; Guarini, G.; Mazzanti, F. Predicting the initial rate of water absorption in clay bricks. *Constr. Build Mater.* **2009**, *23*, 2623–2630. [[CrossRef](#)]
14. Kung, J.H. *Frost Durability of Canadian Clay Bricks*, Proceedings of the 7th International Brick Masonry Conference, Melbourne, VI, Australia, 17–20 February 1985; Brick Development Research Institute, University of Melbourne, Department of Architecture and Building: Melbourne, VI, Australia, 1985; pp. 245–251.
15. Hansen, W.; Kung, J.H. Pore structure and frost durability of clay bricks. *Mat. Struct.* **1988**, *21*, 443–447. [[CrossRef](#)]
16. Radeka, M. Značaj karakteristika pora za otpornost materijala pri dejstvu mraza. *Mater. Konstr.* **2007**, *50*, 14–20. (In Serbian)
17. Radeka, M.; Ranogajec, J.; Marinković-Neducin, R.; Ducman, V.; Sever Skapin, A. The effect of the firing temperature of clay roofing tiles on the mechanism of frost action. *Ind. Ceram.* **2010**, *30*, 97–104.
18. Cultrone, G.; Sebastian, E.; Elert, K.; De la Torre, M.J.; Cazalla, O.; Rodriguez-Navarro, C. Influence of mineralogy and firing temperature on the porosity of bricks. *J. Eur. Ceram. Soc.* **2004**, *24*, 547–564. [[CrossRef](#)]
19. Stryzewska, T.; Kanka, S. Forms of Damage of Bricks Subjected to Cyclic Freezing and Thawing in Actual Conditions. *Materials* **2019**, *12*, 1165. [[CrossRef](#)] [[PubMed](#)]
20. Ducman, V.; Sever Škarpin, A.; Radeka, M.; Ranogajec, J. Frost resistance of clay roofing tiles: Case study. *Ceram. Int.* **2011**, *37*, 85–91. [[CrossRef](#)]
21. Oti, J.E.; Kinuthia, J.M.; Bai, J. Freeze-thaw of stabilised clay brick. *Waste Res. Manag.* **2010**, *163*, 129–135. [[CrossRef](#)]
22. Al-Jaberi, Z.; Ghani, A.; Myers, J.J.; ElGawady, M. *Ability to Resist Different Weathering Actions of Eco-Friendly Wood Fiber Masonry Blocks*, Proceedings of the 16th International Brick and Block Masonry Conference, Padova, Italy, 26–30 June 2016; CRC Press: London, UK, 2016; pp. 883–888.
23. Elert, K.; Culturone, G.; Rodriguez-Navarro, C.; Pardo, E.S. Durability of bricks used in the conservation of historic buildings—Influence of composition and microstructure. *J. Cult. Herit.* **2003**, *4*, 91–99. [[CrossRef](#)]
24. Coletti, C.; Culturone, G.; Maritan, L.; Mazzoli, C. How to face the newindustrial challenge of compatible, sustainable brick production: Study of various types of commercially available bricks. *Appl. Clay Sci.* **2016**, *124–125*, 219–226. [[CrossRef](#)]
25. *Pune Glinene Opeke. Tehnički Uvjeti*; HRN B.D8.011:1987; Croatian Standard Institute: Zagreb, Croatia, 1987. (In Croatian)
26. *Methods of Test for Masonry Units—Part 1: Determination of Compressive Strength*; EN 772-1:2011+A1:2015; European Committee: Brussels, Belgium, 2015.
27. Sveda, M. The effect of firing temperature and dwell time on the frost resistance of a clay roofing tile. *Ziegelind. Int.* **2004**, *5*, 36–40.
28. Brosnan, A. Testing and Freeze-Thaw Durability Prediction for Clay Bricks. *Int. J. Adv. Res. Technol.* **2014**, *3*, 1270–1275.
29. Netinger Grubeša, I.; Marković, B.; Vračević, M.; Tunkiewicz, M.; Szenti, I. Pore Structure as a Response to the Freeze/Thaw Resistance of Mortars. *Materials* **2019**, *12*, 3196. [[CrossRef](#)]

30. Mallidi, S.R. Application of mercury intrusion porosimetry on clay bricks to assess freeze-thaw durability—A bibliography with abstracts. *Constr. Build. Mat.* **1996**, *10*, 461–465. [[CrossRef](#)]
31. Netinger Grubeša, I.; Vračević, M.; Ranogajec, J.; Vučetić, S. Influence of Pore-Size Distribution on the Resistance of Clay Brick to Freeze–Thaw Cycles. *Materials* **2020**, *13*, 2364. [[CrossRef](#)] [[PubMed](#)]
32. Korat, L.; Ducman, V.; Legat, A.; Mirtič, B. Characterisation of the pore-forming process in lightweight aggregate based on silica sludge by means of X-ray micro-tomography (micro-CT) and mercury intrusion porosimetry (MIP). *Ceram. Int.* **2013**, *39*, 6997–7005. [[CrossRef](#)]



© 2020 by the authors. Licensee MDPI, Basel, Switzerland. This article is an open access article distributed under the terms and conditions of the Creative Commons Attribution (CC BY) license (<http://creativecommons.org/licenses/by/4.0/>).